Orbital selectivity in the normal state of KFe(2)Se(2) superconductor

To cite this article before publication: Luis Craco *et al* 2021 *EPL* in press https://doi.org/10.1209/0295-5075/ac3f16

epl draft

Orbital selectivity in the normal state of KFe_2Se_2 superconductor

L. Craco[1,2] and S. Leoni[3]

[1] *Institute of Physics, Federal University of Mato Grosso, Cuiabá, MT 78060-900, Brazil*
[2] *Leibniz Institute for Solid State and Materials Research Dresden, Helmholtzstr. 20, D-01069 Dresden, Germany*
[3] *School of Chemistry, Cardiff University, Cardiff, CF10 3AT, UK.*

PACS 31.15.A – Ab initio calculations
PACS 71.10.Fd – Lattice fermion models (Hubbard model, etc.)
PACS 71.30.+h – Metal-insulator transitions and other electronic transitions

Abstract. - Using density functional dynamical mean-field theory, we show how correlation effects lead to pseudogap and Kondo-quasiparticle features in the electronic structure of pure and doped KFe_2Se_2 superconductor. Therein, correlation- and doping-induced orbital differentiation are linked to the emergence of an incoherent-coherent crossover in the normal state of KFe_2Se_2 superconductor. This crossover explains the puzzling temperature and doping dependent evolution of resistivity and Hall coefficient, seen in experiments of alkali-metal intercalated iron-selenide superconductors. Our microscopic description emphasises the role of incoherent and coherent electronic excitations towards unconventional transport responses of strange, bad-metals.

Introduction. – The finding of high-temperature (high-T_c) superconductivity on the border of striped antiferromagnet in Fe-pnictides and chalcogenides led to renewed activity in the field of unconventional superconductivity [1]. Due to telling similarities with cuprate-oxide superconducting (SC) materials [2], Fe-based superconductors are being considered within different interpretation frameworks. Central to this debate are the questions, whether Fe-pnictides and chalcogenides are weakly correlated Fermi-liquid (FL) metals, or whether they lie in close proximity to a correlation-driven Mott insulator. Despite its fundamental importance, the resolution of this issue and the consequent description of the normal electronic state properties have proved difficult for both c uprates and Fe-based superconductors. This can be ascribed to the multi-band (cuprates) and multi-orbital (Fe-superconductors) character of both SC compound classes. Of particular interest for the Mottness [3] scenario are alkali-metal iron-selenide superconductors [4], due to their proximity to Mott metal-insulator instabilities [5–7].

The discovery of superconductivity in tetragonal KFe_2Se_2 [8] is of particular interest since it appears in the parent compound [9], without any need for Fe/chalcogen composition tuning [10] or intercalation chemistry [11]. A natural question concerns therefore the orbital-selective nature [6] of the low-energy electronic states in this and its derivative compounds, which also host a metal-to-SC phase instability and a normal state with insulating-like behavior above a characteristic temperature [12]. Here, we provide insights to this fundamental problem showing that the KFe_2Se_2 parent compound is an incoherent metal in close proximity to an orbital-selective insulating state.

$A_xFe_{2-y}Se_2$ ($A = K,\ Rb$) superconductors also offer an alternative platform for the study of orbital-selective Mott physics [6,7] and the linear-in-T resistivity [13,14] of strange-metals [15]. We recall here that the normal state of a large class of correlated materials, including high-T_c superconductors, often falls into the strange-metal category, where the resistivity varies linearly with temperature as $T \to 0$. This together with strongly T-dependent Hall effect (see our discussion below) represent significant deviations from the conventional FL picture of metals. Although the fundamental origin for this anomalous, non-FL behavior [16] is still under debate [17], it seems that the underlying key mechanism is Mottness [3], i.e. the proximity of strongly correlated materials to a Mott transition. On more general grounds the strange-metal phase exhibits a nonsaturating, T-linear electrical resistivity, due to vanishing quasiparticle weight in the normal state: Examples of systems showing pseudogap features and absence of electron quasiparticles include Cu-oxide and Fe-based superconductors as well as heavy fermion materials near a quantum critical point. In this work we partially confirm the linear-in-T behavior seen on different experimental conditions [13, 14], showing that it can be tuned via hole doping the KFe_2Se_2 parent compound.

Magnetotransport measurements provide important information concerning the temperature dependence of charge-carrier densities and electron mobilities in different bands in the normal and *SC* phases [18, 19]. Extant magnetotransport measurements reveal that the Hall coefficient of $K_xFe_{2-y}Se_2$ is negative over the whole temperature range [12,19], indicating that these systems are dominated by electron-like charge carriers [20]. (This behavior is in accordance with the observation of electron Fermi pockets in ARPES measurements [7]). Motivated thereby we undertake a local density approximation plus dynamical mean-field theory (LDA+DMFT) [21] study of the Hall coefficient in pure and doped KFe_2Se_2. Consistent with experimental data [19], our results reveal a non-monotonic T-dependence of the Hall response. Thus, we confirm previous experimental evidences suggesting that the exotic T-dependent behavior of the Hall response cannot be described by a single-band model [19], and the need of including multiband electronic correlations in alkali-metal iron-selenide superconductors.

It should be noted that the $K_xFe_{2-y}Se_2$ system separates into two phases [8], particularly upon thermal treatment during single crystal growth [13, 22]. This results into a minor *SC* phase and a major non-*SC* phase [9, 23], referred to as 245 [24]. Because of such a microscopic phase separation [25], it has been difficult to elucidate intrinsic physical properties of the *SC* phase and its pairing mechanism. A perusal of extant literature suggests that both mesoscopic phase separation and *SC* properties can be tuned by an appropriate control of the quenching process. While slow cooling leads to a 12% *SC* phase with $T_c \approx 44$ K, faster quenching rate seems to lead to a suppression of formation of the non-*SC* 245 phase up to 50%, inducing a monotonic reduction in the *SC* T_c from 30.7 to 26.0 K [22]. It has been also suggested that the stoichiometric *SC* phase with $I4/mmm$ symmetry persists below a disorder-to-order transition at $T_S \approx 580$ K concomitantly with the emergence of a nonstoichiometric phase with a lower $I4/m$ lattice symmetry in which the Fe vacancies undergo long-range order [23]. Moreover, in the 245 Mott insulating phase [5] an antiferromagnetic transition occurs following the structural one at $T_N \approx 560$ K [26]. Thus an important issue in this material class has been to understand whether competing interactions lead to phase separation of *SC* from non-*SC* Mott localized domains. In this work we shed light to this problem showing that the stoichiometric KFe_2Se_2 superconductor is in close proximity to orbital-selective Mott localization and that the coherent-incoherent crossover seen in transport [12,13,22,23] is an intrinsic property of the *SC* phase and the two-particle fingerprint of selective Mottness of strongly correlated Fe-chalcogenide superconductors.

Theory and discussion. – We focus on the parent KFe_2Se_2 system without mesocopic phase separation [13, 22, 23], since the issue related to additional increase in electronic localization associated with Fe-vacancy order in

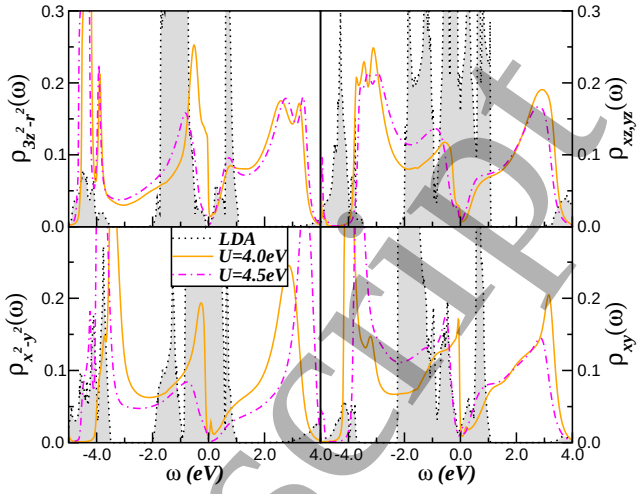

Fig. 1: Orbital-resolved LDA+DMFT density-of-states (DOS) for the Fe $3d$ orbitals of KFe_2Se_2 near the Mott metal-insulator transition. The LDA DOS is shown for comparison.

$KFe_{1.6}Se_2$ was already studied within MO LDA+DMFT in Ref. [5]. However, if we aim to understand material specific properties of stoichiometric KFe_2Se_2 superconductor it is important to identify the character of dominant bands near the Fermi level and their energy distribution. To this purpose *ab initio* density-functional theories (DFT) are the best tools available. Our local density approximation (LDA) result [27] in Fig. 1 confirms previous calculations on Fe-chalcogenide [28] and arsenide systems [29] showing that the dominant states near the Fermi level come from Fe-$3d$ atomic states extending roughly between -2 eV to 1 eV for KFe_2Se_2. Hence, from LDA the one-electron part the MO Hamiltonian for KFe_2Se_2 is $H_0 = \sum_{\mathbf{k},a,\sigma} \epsilon_a(\mathbf{k}) c^{\dagger}_{\mathbf{k},a,\sigma} c_{\mathbf{k},a,\sigma}$, where $a = 3z^2 - r^2, xz, yz, x^2 - y^2, xy$ label the diagonalized five $3d$ bands and $\epsilon_a(\mathbf{k})$ is the one-electron band dispersion, which encodes details of the bare band structure of KFe_2Se_2. However, in order to provide the appropriate microscopic framework for the metallic state in the Fe-based superconductors a consistent description of electron correlation effects and the role played by electron/hole doping is required. This fundamental issue becomes especially relevant to disorder-free MO systems, where the bad-metallic regime arises from the scattering between Mott localized and itinerant electronic states hidden in the correlated MO problem. We use LDA+DMFT to study the emergence of a reconstructed electronic structure in KFe_2Se_2, showing that its normal state is intrinsically a pseudogap-metal, which is induced by dynamical MO correlations encoded in the many-particle Hamiltonian $H_{int} = U \sum_{i,a} n_{ia\uparrow} n_{ia\downarrow} + U' \sum_{i,a\neq b} n_{ia} n_{ib} - J_H \sum_{i,a,b} \mathbf{S}_{ia}.\mathbf{S}_{ib}$. Here, U and $U' = U - 2J_H$ are the intra- and inter-orbital Coulomb repulsion and J_H is the Hund's rule coupling [21]. It is worth noting here that earlier studies on alkali metal iron-selenides undertake LDA+DMFT

calculations using $U = 3.5$ eV and $0.56 \leq J_H \leq 0.7$ eV as model parameters for $K_{1-x}Fe_{2-y}Se_2$ [30]. An $U = 3.75$ eV has also been introduced by M. Yi *et al.* [7] in their study of temperature-induced crossover in $A_xFe_{2-y}Se_2$ (A=K,Rb) *SC* systems. This on-site Coulomb interaction parameter was also used by Nekrasov *et al.* in their quantum Monte Carlo (QMC), LDA'+DMFT study on electron correlation effects in $K_{1-x}Fe_{2-y}Se_2$ superconductors [31]. However, consistent with our early study on unconventional Mott transition in $KFe_{1.6}Se_2$ [5] where good qualitative agreement with transport (*dc* and *ac*) data were obtained using $U = 4.0$ eV and J_H=0.7 eV, we use these as representative model parameters for pure and doped KFe_2Se_2 superconductor. While the absolute value of the on-site intra- and inter-orbital Coulomb interactions are sensitive to bare LDA input, like the number of bands considered in the LDA Hamiltonian [31] or the effect of various possible screening channels on the value of the effective on-site Hubbard interaction [32], our choice here is consistent with earlier studies mentioned above. Finally, we use the MO iterated perturbation theory (MO-IPT) as an impurity solver for DMFT [33].

To gain realistic insights into the correlated $3d$ electronic structure of KFe_2Se_2 parent compound in Fig. 1 we compare the orbital-resolved spectral function obtained within LDA and LDA+DMFT calculations. At commensurate electron filling $n = 6.0$ per Fe (corresponding to Fe^{2+} valance state of the parent compound) a substantial electronic reconstruction is obtained for the Fe-$3d$ states at the border of the orbital-selective Mott phase [7] for KFe_2Se_2. Dynamical MO correlations originating from $U = 4.0$ eV ($U' = 2.6$ eV) and $J_H = 0.7$ eV lead to spectral weight redistribution over large energy scales and the formation of a reconstructed (compared to LDA) electronic structure. This feature is characteristic of MO Mott-Hubbard systems, with concomitant emergence of upper and lower Hubbard bands at high-energies: These latter features are related to coupled local moments [34] defining a system close to a Mott insulator without long-range vacancy or magnetic ordering [23]. Furthermore, with increasing U from 4.0 to 4.5 eV the electronic states close to E_F are transferred to higher energies, i.e., towards to the Hubbard bands. As a result the Mott-Hubbard insulating gap sets in at E_F. Important as well are the shoulder structures above the leading edges at binding energies between 0.4 and 0.8 eV which are fingerprints of MO electron-electron interactions already probed in ARPES for $K_{0.8}Fe_2Se_2$ [35].

We turn now to a comparison between our LDA+DMFT result for $U = 4.0$ eV and $J_H = 0.7$ eV with another approach which uses quantum Monte Carlo (QMC) to solve the impurity problem of DMFT [31]. First, we see in Fig. 4 that the QMC calculation resolve a peak near E_F in the $3z^2 - r^2, xy$ orbitals. Though V-shaped pseudogaps can be discerned in the xz, yz and $x^2 - y^2$ orbitals in Ref. [31], a direct comparison between LDA'+DMF(QMC) [31] and LDA+DMFT(MO-IPT) results show that the many-body renormalized QMC DOS is metallic and close to the bare LDA and LDA' DOS. Our result however is near to orbital-selective Mott localization in good quantitative accord with coherent-incoherent crossover behavior in transport for electron doped KFe_2Se_2 as discussed below. What are the sources of the discrepancy between our result and the LDA'+DMFT(QMC) one? There are several important differences between our approach compared to the LDA'+DMFT(QMC). The LDA'+DMFT(QMC) study derive the many-body DOS of the Fe $3d$ orbitals using the full LDA Hamiltonian, which includes all Fe-$3d$, Se-$4p$, K-$4s$ states. While using slightly different U values and bare one-particle inputs to DMFT, our comparison in Fig. 4 suggests that incorporation of Se-$4p$ and K-$4s$ states in the multiband and MO problem of tetragonal KFe_2Se_2 superconductor leads to a d-band model with an effective bandwidth that is enhanced relative the starting bare $3d$ bandwidth (W) of the Fe-$3d$ shell. Correlation-induced spectral weight transfer from low to high energies is expected to enhance the pd and sd hybridizations, leading to an effective screened Coulomb interaction in the correlated subspace. Future all-electron DFT+DMFT calculations should consider intrinsic screening effects [32] as well as the importance of incorporating within the same theoretical framework stronger electronic correlations in all active band states.

In view of large spectral weight transfer manifested in strongly correlated electron systems, one should ask what happens upon (electron/hole) doping a bad-metal at the verge of a MO Mott instability? Even though data exists for $K_xFe_{2-y}Se_2$ systems [4, 7, 35], the generic appearance

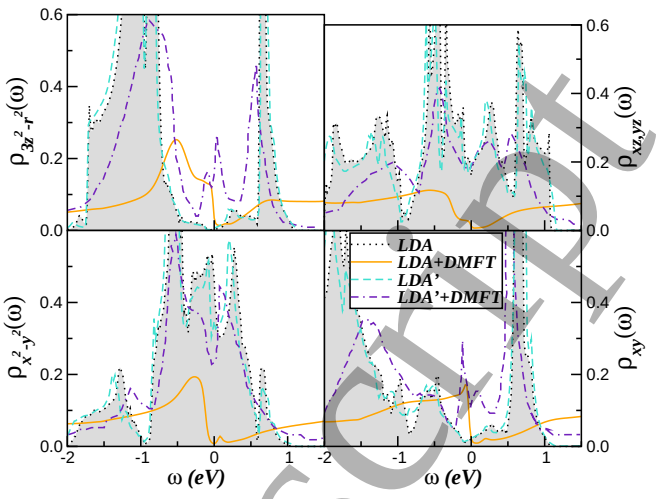

Fig. 2: Orbital-resolved DOS for the Fe $3d$-orbitals of stoichiometric KFe_2Se_2 superconductor, computed using quantum Monte Carlo (QMC, for $U = 3.75$ eV and $J_H = 0.6$ eV) [31] and multi-orbital iterated perturbation theory (MO-IPT, for $U = 4.0$ eV and $J_H = 0.7$ eV). In spite of similar model parameters and bare DOS, strong electron localization is found within MO-IPT as compared to the QMC result. As visible the orbital-resolved LDA' DOS [31] is close to bare LDA one.

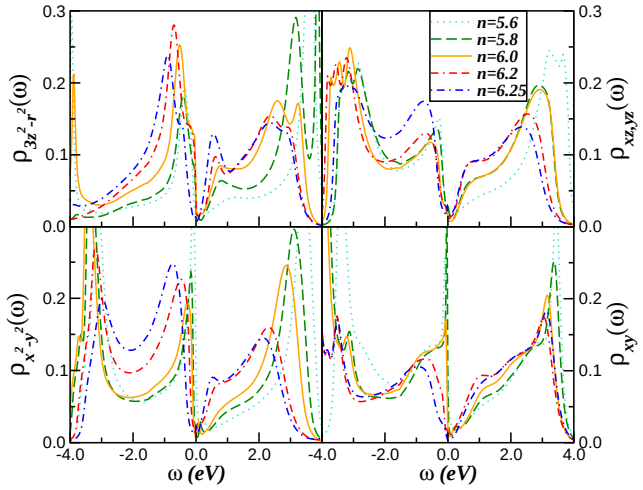

Fig. 3: Orbital-resolved LDA+DMFT DOS for the Fe d orbitals of pure ($n = 6.0$) and doped ($n = 6.0 \pm \delta$) KFe_2Se_2 superconductor. Large spectral weight transfer upon changes of electron concentration (n) along with coexistence selective pseudogap features and narrow Kondo-quasiparticles is visible.

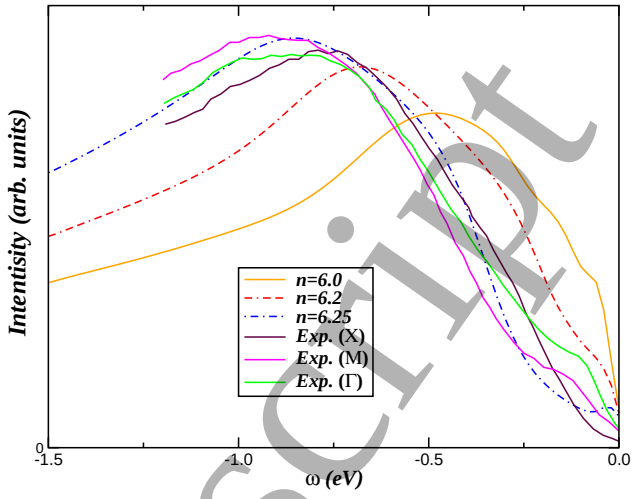

Fig. 4: Comparison between the LDA+DMFT results for pure and doped KFe_2Se_2 and ARPES of $K_{0.8}Fe_{1.7}Se_2$ superconductor ($T_c = 30$ K) recorded at high symmetry points in Ref. [41]. Good semi-quantitative agreement is seen for $n = 6.25$. In particular, the low-energy energy spectrum and the peak at -0.87 eV in ARPES at M and Γ poits are resolved in the total LDA+DMFT spectrum with $U = 4.0$ eV and $J_H = 0.7$ eV.

of novel metallic states and the instabilities of such states to unconventional order in a variety of other correlated materials makes this a very important question to inquire about. With this in mind, in Fig. 3 we show the changes in the correlated electronic structure upon electron/hole doping ($n \equiv 6 \pm \delta$) the parent compound KFe_2Se_2, $\delta = 0$. An intriguing observation in Fig. 3 is that the localization-delocalization transition does not occur simultaneously in all orbitals at small doping. However, as δ increases to negative values, an emergent orbital differentiation starts to develop, in which the $xz, yz, 3z^2 - r^2$ spectral functions show pseudogap-like behavior with vanishing DOS at E_F while the $x^2 - y^2, xy$ orbitals show (selective) metallic behavior, characterized by the many-body stabilization of narrow Kondo quasiparticles near E_F. Interestingly, this behavior is in good accord with the observation of spectral weight transfer from the high- to low-energy region and the formation of a coherent peak in the d_{xy} orbital of KFe_2As_2 [36]. Thus, consistent with earlier correlated band structure calculations for KFe_2As_2 [36] as well as with photoemission spectroscopy studies of LiFeAs [37], our results for hole doped KFe_2Se_2 suggest a common underlying scenario where the d_{xy} DOS sharpens at low temperatures and dominates the low-energy one-particle spectra, signaling an emergent orbital differentiation in this and related Fe-based SC systems [38].

Since there is no particle-hole symmetry in the d^6 electronic configuration of Fe-based superconductors, it is interesting to inquire as to the effects of electron doping KFe_2Se_2 superconductor. In particular, does the incoherent non-FL behavior for $n = 6.0$ survives in the infrared region? Fig. 3 exhibits the answer to this question. As seen, increasing electron concentration ($\delta > 0$) drives stoichiometric KFe_2Se_2 to a phase where the $x^2 - y^2, xy$ orbitals lose their spectral weight near E_F while the other orbitals remain incoherent. This is a demonstration of an orbital-selective bad-metal reconstruction in electron doped KFe_2Se_2 with overdamped collective modes at low energies. In accord with earlier studies [5,39], the increase of the effective U/W ratio (W is the LDA bandwidth) in the present case relative to tetragonal FeSe [38], due to intercalation of potassium ions into the interstitial site between the FeSe layers, leads to increased low-energy incoherence with pronounced pseudogap features at low energies. Microscopically, incoherent scattering arising from orbital-selective bad-metallic states leads to a suppression of the infrared FL behavior (narrow Kondo-quasiparticles in DMFT) and the emergence of a pseudogaped spectra, reminiscent of what is seen in the paramagnetic normal state of tetragonal Fe-chalcogenide systems [4,40].

To investigate further the electronic structure reconstruction of KFe_2Se_2 upon electron doping, in Fig. 3 we compare our $U = 4$ eV (and, $U' = 2.6$ eV) results with angle-resolved photoemission spectroscopy (ARPES) for $K_{0.8}Fe_{1.7}Se_2$ recorded at high symmetry points in Ref. [41]. As seen, good semi-quantitative agreement with experiment is obtained for $n = 6.25$. In particular, the broad peak close to -0.87 eV as well as the detailed form of the lineshape in ARPES is well reproduced by the LDA+DMFT result for the electron doped case. This may suggest that the experiment could have been done on a tetragonal sample with similar incoherent electronic structure as we derive here for $n = 6.25$. For comparison, the computed total LDA+DMFT spectra for the undoped

($n = 6.0$) and electron doped ($n = 6.2$) cases show progressively more disagreement with ARPES at the energy window relevent to Ref. [41]. However, it is worth noting that the shoulder feature close to 0.45 eV binding energy and the low-energy pseudogap we obtain for $n = 6.0$ are robust features seen in ARPES for $K_{0.8}Fe_2Se_2$ [35], providing additional support to our LDA+DMFT study.

In an earlier study [5] it was shown that the unconventional transport properties of electron doped $KFe_{1.6}Se_2$ can be understood using LDA+DMFT with sizable d band correlations. Here, we extend this to characterize the electronic and magnetotransport behavior of pure and doped KFe_2Se_2. Specifically, in addition to dc resistivity [$\rho_{dc}(T)$], we show how the Hall constant [$R_H(T)$] is also described, and correlate with the evolution of the DMFT spectral functions, $A_a(\omega)$. Within the DMFT formalism the dc-conductivity can be expressed as $\sigma_{xx}(T) = \pi e^2 v^2 \sum_a \int d\epsilon \rho_a^{(0)}(\epsilon) \int d\omega A_a^2(\epsilon,\omega)[-f'(\omega)]$ [42], where $\rho_a^{(0)}(\epsilon)$ is the LDA DOS of the five $3d$-bands, v is the electron's velocity and $f(\omega)$ is the Fermi function. Noteworthy, as in Ref. [43] the only approximation made here is to ignore the $\mathbf{k}$ and orbital dependence of the electron's velocities $v_a(\mathbf{k})$, i.e, $v_a(\mathbf{k}) \to v_a = v$. In an incoherent metal close to Mottness, such as we have here, this is justified, since, between successive hops, a carrier in an incoherent state does not exist long enough in a given (band) $\mathbf{k}$ eigenstate. Another compelling reason for justifying this approximation is that different sources of scattering, neglected in our LDA+DMFT formulation but present in reality, like phonons, microscopic phase separation, and lattice defects, will partially degrade the quasiparticle momentum. In this situation, following Saso *et al.* [44], we approximate the $v_a(\mathbf{k})$ by a single average carrier velocity v for all orbitals. In fact, Saso *et al.* [44] and Baldassare *et al.* [45] have shown that this assumption works well for Kondo insulators (FeSi and YbB_{12}) as well as for V_2O_3, supporting our approximation for the fermions's velocities. Moreover, for the computation of Hall conductivity [$\sigma_{xy}(T)$] we have generalized the DMFT formalism [42] to the five-orbital case relevant for KFe_2Se_2, which reads $\sigma_{xy}(T) = \frac{\pi^2|e|^3v^2}{3} H \sum_a \int \epsilon d\epsilon \rho_a^{(0)}(\epsilon) \int d\omega A_a^3(\epsilon,\omega)[-f'(\omega)]$, with H being the magnetic field. The observed features in resistivity $\rho_{dc}(T) = 1/\sigma_{xx}(T)$ and Hall coefficient [46] $R_H(T) = \frac{\sigma_{xy}(T)}{H\sigma_{xx}^2(T)}$ originate from doping induced spectral changes, showing how this provides a qualitative description of extant experimental data is our focus below.

With this in place, let us now discuss our resistivity results for pure and electron/hole doped KFe_2Se_2. The T-dependence of $\rho_{dc}(T)$ upon smal changes in the total band filling n of the Fe $3d$-shell is shown in Fig. 5. In the hole doped regime with $n = 5.6$ the resistivity shows the S-like shape characteristic of pseudogap metals [47], and it is similar to the in-plane resistivity behavior of Sr-doped cuprates [48]. Interestingly, our result for $n = 5.6$ shows almost linear-in-T behavior above 80 K conisitent with that seen in quenched [14] and in a particular normal

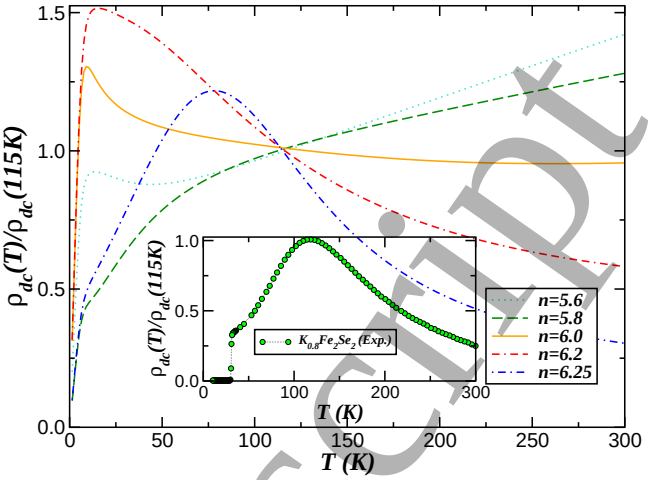

Fig. 5: Resistivities of pure and doped KFe_2Se_2 as a function of temperature for $U = 4.0$ eV and $J_H = 0.7$ eV. Inset display the transport data taken from Ref. [12]. Particularly interesting is the broad hump (around 115 K) indicating a semiconducting-to-metal crossover. Although at different temperatures this coherence-incoherence crossover behavior observed in experiment is well reproduced by LDA+DMFT for $n = 6.25$.

state regime of granular [13] $KFe_{2-y}Se_2$ superconductor. In going from $n = 5.6$ to $n = 5.8$ the system becomes more conductive as a result of strong orbital reconstruction of the electronic states at low energies, indicating a smooth deviation from power law form outside the strange-metal regime. However, as shown in Fig. 5 at low T the FL-like T^2 form is never observed in our resistivity curves. Moreover, for $n \geq 6.0$ a T-dependent crossover from an insulator to a low-T bad metal is obtained. Clearly, this crossover scale is marked by the maximum of $\rho_{dc}(T)$; for $n = 6.2$ it yields an insulating-like behavior above 15 K. Additionally, our theory-experiment comparison in the inset of Fig. 5 demonstrates that the T-dependence of the LDA+DMFT result for $n = 6.25$ (a total band filling also discussed in Ref. [49]) is in qualitative good accord with experimental data for $K_{0.8}Fe_2Se_2$ [12] albeit at lower T. As in experiment, our resistivity curve for $n = 6.25$ shows no sign of saturation at high temperature, although saturating metal physics similar to that found for n between 5.6 and 6.0 has been found in transport experiments of $K_xFe_{2-y}Se_2$ under different quenching conditions [13].

Finally, we turn our attention to the effect of electron/hole doping on the T-dependence of the Hall coefficient, $R_H(T)$. We recall here that Hall measurements provide valuable informations regarding the T-dependence of the charge-carrier density and mobilities of electrons on different bands in the normal and SC states [19]. For good metals with FL coherence $R_H(T)$ is constant [50], but it can have anomalous behavior in cuprates [51] and in Fe-based superconductors [12, 18, 19, 52]. While for $NdFeAsO_{1-x}F_x$ ($x = 0.0, 0.18$) $R_H(T)$ decay continuously

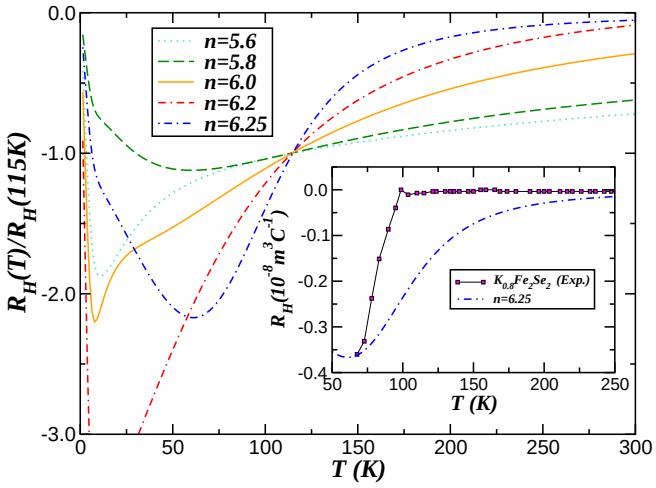

Fig. 6: The temperature dependence of the Hall coefficient for pure and doped KFe_2Se_2 calculated using the LDA+DMFT orbital resolved spectral functions. The inset shows the experimental result for $K_{0.8}Fe_2Se_2$ [12] in the normal state. (The theory curve was rescaled to coincide with experiment at 67 K.)

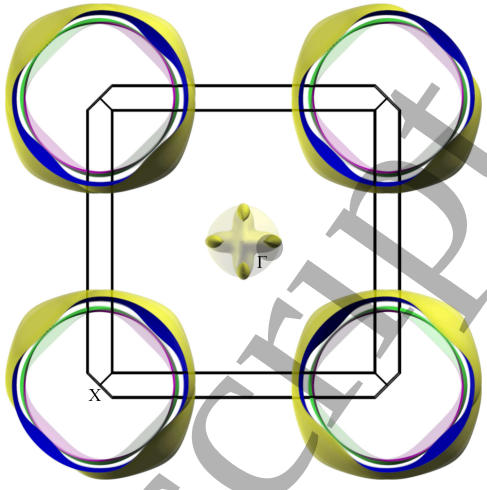

Fig. 7: Fermi isosurfaces interpolated at the corresponding Fermi level values for $U = 0$ (LDA), 6 and 7 eV. More opaque surfaces correspond to higher U values. For $U = 6$ eV, the pristine LDA spherical region is distorted into connected lobes (*propeller*), followed by a topolgical change on further increasing $U = 7$ eV, with the formation of four disconnected lobes, aligned at 45 ∘ with respect to the Γ to X direction.

with increasing temperature [18], in $K_{0.8}Fe_2Se_2$ $R_H(T)$ is almost constant above 100 K and decays linearly with decreasing T in the normal state. It is also worth noting that the linear-in-T behavior reported by Guo *et al.* [12] for $K_{0.8}Fe_2Se_2$ is in contrast to that of $K_xFe_{2-y}Se_2$ single crystals [19], where the Hall coefficient show nonlinear behavior below 60 K and decreases almost linearly above 80 K. Interestingly, as shown in the main panel of Fig. 6, $R_H(T)$ shows clear nonmonotonic T-dependence and it is negative over the whole temperature region up to 300 K, confirming as in experiments that the conduction of K-intercalated iron-selenide is mostly dominated by electron-like charge carriers. Additionally, in the inset of this figure we provide a direct theory-experiment comparison, showing that the relative magnitude between low- and high-T data of $K_{0.8}Fe_2Se_2$ [12] is well reproduced within LDA+DMFT for $n = 6.25$. However, the most remarkable feature of our results in Fig. 6 is the T-dependence of R_H for $n = 6.0$, which resembles that seen in the normal state of $Tl_{0.64}K_{0.36}Fe_{1.83}Se_2$ system [20] as well as of $Rb_xFe_2Se_2$ below 100 K [53]. Taken theory and experiment together, our LDA+DMFT results of pure and (electron/hole) doped KFe_2Se_2 seem to suggest that the different behaviors in magnetotransport data discussed above might be related to intrinsic orbital-selective Mott physics which can be probed differently as a consequence of sample preparation [19] or electronic phase separation [54].

Fermi Surface Topology. – Correlation is believed to cause a complicated structuring of the Fermi surface (FS) in proximity of Γ-point, as indicated by experiment and further supported by DMFT approaches [30]. The departure from a spherical shape and correlation-driven reshaping of the innermost FS sheet are creating a so-called hidden hole-like surface near Γ-point [30]. Therefore, to further probe the role of electronic correlations, we have determined the on-site Hubbard U in stoichiometric KFe_2Se_2 [55], using an approach based on density-functional perturbation theory (DFPT) [56]. The resulting $U = 7.0$ eV indicates sizeable correlation in KFe_2Se_2. Fermi surfaces calculated at different U values ($U = 0.0$ eV (LDA), 6.0 eV and 7.0 eV) shows the onset of distortion of the pristine spherical pocket (LDA) into connected lobes, which become fully disconnected at $U = 7.0$ eV, as shown in Fig. 7. This topological change is therefore purely a consequence of correlation, which is driving the FS reshaping away from the LDA scenario of a fully connected Fermi pocket at Γ-point. This pinpoints the important role of sizeable correlation on transport properties in this compound class, further modulated by multiorbital contributions, as shown in the detailed LDA+DMFT study above.

Conclusion. – To conclude, based on a LDA+DMFT study, we have shown that orbital-selective incoherence characterizes the paramagnetic normal phase of KFe_2Se_2 superconductor. Good qualitative agreement with experimental data and rationalization of a variety of unusual observations in electrical- and magneto-transport within a single theoretical picture lend support to our proposal. The emergence of a semiconducting-to-metal crossover at finite temperatures seen in experiments of $K_xFe_{2-y}Se_2$ superconductor [12, 13, 23, 26] should be considered as a multi-orbital manifestation of slightly increasing the band filling via electron doping an orbital-selective bad-metal in close proximity to Mott localization. Increasing Mottness upon electron-doping the KFe_2Se_2 parent compound

suggests a promising and practical route to access quantum critical physics [57] in 122 Fe-chalcogenide systems. On the other hand, at small hole doping we predict an orbital differentiation phenomena, where d_{xy} density-of-state sharpens at low temperature and dominates the low-energy spectral function of KFe_2Se_2. This behavior is consistent with the appearance of a coherent d_{xy} peak in the DFT+DMFT density-of-states at the Fermi level in the hole-overdoped KFe_2As_2 [36] as well as with observations in angle-resolved photoemission spectroscopy of quasiparticles with d_{xy} orbital character in LiFeAs [37] and strong renormalization in the d_{xy} bands of $FeTe_{0.56}Se_{0.44}$, monolayer $FeSe/SrTiO_3$ and $K_{0.76}Fe_{1.72}Se_2$ [58], placing our findings for KFe_2Se_2 superconductor in a broader context.

* * *

L.C. is supported by CNPq (Grant No. 304035/2017-3). Acknowledgment (L.C.) is also made to CAPES. S.L. thanks ARCCA Cardiff for computational resources.

REFERENCES

[1] Si, Q., Yu, R. and Abrahams, E., *Nature Rev. Mater.*, **1** (2016) 16017.
[2] Ye, C. *et al.*, *Phys. Rev. X*, **5** (2015) 021013.
[3] Choy, T. P. and Phillips, P., *Phys. Rev. Lett.*, **95** (2005) 196405.
[4] Dagotto, E., *Rev. Mod. Phys.*, **85** (2013) 849.
[5] Craco, L., Laad, M.S. and Leoni, S., *Phys. Rev. B*, **84** (2011) 224520.
[6] Yu, R. *et al.*, *Frontiers in Physics*, **9** (2021) 578347.
[7] Yi, M. *et al.*, *Phys. Rev. Lett.*, **110** (2013) 067003.
[8] Li, W. *et al.*, *Nature Phys.*, **8** (2012) 126;
[9] Li, W. *et al.*, *Phys. Rev. Lett.*, **109** (2012) 057003.
[10] Berlijn, T. *et al.*, *Phys. Rev. B*, **89** (2014) 020501(R).
[11] Vivanco, H.K. and and Rodriguez, E.E., *J. Solid State Chem.*, **242** (2016) 3.
[12] Guo, J. *et al.*, *Phys. Rev. B*, **82** (2010) 180520(R).
[13] Soares, C.C. *et al.*, *Sci. Rep.*, **8** (2018) 7041.
[14] Tanaka, M. *et al.*, *J. Phys. Soc. Jpn.*, **85** (2016) 044710.
[15] Anderson, P.W., *Nature Phys.*, **2** (2006) 626.
[16] Stewart, G.R., *Rev. Mod. Phys.*, **73** (2001) 797.
[17] Andrade, T. *et al.*, *Nature Phys.*, **14** (2018) 1049.
[18] Cheng, P. *et al.*, *Phys. Rev. B*, **78** (2008) 134508.
[19] Ding, X. *et al.*, *Phys. Rev. B*, **89** (2014) 224515.
[20] Fang, M.-H. *et al.*, *Europhys. Letts.*, **94** (2011) 27009.
[21] Kotliar, G. *et al.*, *Rev. Mod. Phys.*, **78** (2006) 865.
[22] Yanagisawa, Y. *et al.*, *J. Phys. Soc. Jpn.*, **86** (2017) 043703.
[23] Yang, J. *et al.*, *Phys. Rev. B*, **94** (2016) 024503.
[24] Wang, C.-H. *et al.*, *Proc. Natl. Acad. Sci. USA*, **116** (2019) 1104.
[25] Chen, Y. *et al.*, *Nano Res.*, **14** (2021) 823.
[26] Yan, Y.J. *et al.*, *Sci. Rep.*, **2** (2012) 212.
[27] Within the tetragonal (space group: $I4/mmm$) structure of $K_xFe_2Se_2$ and lattice parameters derived in Ref. [12], one-electron band structure calculations based on LDA have been performed for KFe_2Se_2 using the linear muffin-tin orbitals (LMTO) scheme. The radii of the atomic spheres were chosen as r=2.6 a.u. (Fe), r=4.25 a.u. (K) and r=2.7 a.u. (Se) [5] in order to minimize their overlap.
[28] Subedi, A. *et al.*, *Phys. Rev. B*, **78** (2008) 134514.
[29] Haule, K., Shim, J.H. and G. Kotliar, G., *Phys. Rev. Lett.*, **100** (2008) 226402.
[30] Nekrasov, I.A., Pavlov, N.S. and Sadovskii, M.V., *JETP Letters*, **108** (2018) 623.
[31] Nekrasov, I.A., Pavlov, N.S. and Sadovskii, M.V., *JETP*, **117** (2013) 926.
[32] Aryasetiawan, F., Karlsson, K., Jepsen, O. and Schönberger, U., *Phys. Rev. B*, **74** (2006) 125106.
[33] Craco, L., *Phys. Rev. B*, **77** (2008) 125122.
[34] Leonov, I. *et al.*, *Phys. Rev. Lett.*, **115** (2015) 106402.
[35] Zhang, Y. *et al.*, *Nature Mat.*, **10** (2011) 273.
[36] Yang, R. *et al.*, *Phys. Rev. B*, **96** (2017) 201108(R).
[37] Miao, H. *et al.*, *Phys. Rev. B*, **94** (2016) 201109(R).
[38] Craco, L., Laad, M.S. and Leoni, S., *J. Phys.: Conf. Ser.*, **487** (2014) 012017.
[39] Craco, L., Laad, M.S. and S. Leoni, S., *J. Phys.: Condens. Matter.*, **26** (2014) 145602.
[40] Craco, L. and S. Leoni, S., *Sci. Rep.*, **7** (2017) 46439.
[41] Qian, T. *et al.*, *Phys. Rev. Lett.*, **106** (2011) 187001.
[42] Romano, A. and Ranninger, J., *Phys. Rev. B*, **62** (2000) 4066; see also, Haldar, P. *et al.*, *Phys. Rev. B*, **96** (2017) 155113.
[43] Craco, L and Leoni, S., *Sci. Rep.*, **5** (2015) 13772; Craco, L. and Laad, M. S., *Eur. Phys. J. B.*, **89** (2016) 119; Craco, L., da Silva Pereira, T. A., and Leoni, S., *Phys. Rev. B*, **96** (2017) 075118.
[44] Urasaki, K and Saso, T., *J. Phys. Soc. Jpn.*, **68** (1999) 3477; Saso, T., *J. Phys. Soc. Jpn.*, **73** (2004) 2894.
[45] Baldassarre, L *et al.*, *Phys. Rev. B*, **77** (2008) 113107.
[46] Yang, Y.-F., *Phys. Rev. B*, **87** (2013) 045102.
[47] Craco, L. and Laad, M.S., *Eur. Phys. J. B*, **89** (2016) 119.
[48] Takenaka, K. *et al.*, *Phys. Rev. B*, **65** (2002) 092405.
[49] Yin, Z.P., Haule, K. and Kotliar, G., *Nature Mat.*, **10** (2011) 932.
[50] Nair, S. *et al.*, *Advances in Physics*, **61** (2012) 583.
[51] Ong, N.P., *Physical Properties of High-Temperature Superconductors* (edited by D. M. Ginsberg (World Scientific, Singapore, 1990), p. 459).
[52] Lin, H. *et al.*, *Phys. Rev. B*, **93** (2016) 144505.
[53] Luo, X. G. *et al.*, *New J. Phys.*, **13** (2011) 053011.
[54] Bendele, M. *et al.*, *Sci. Rep.*, **4** (2014) 5592.
[55] The DFPT approach to Hubbard U calculations [56] was used as implemented in the Quantum ESPRESSO package (v 6.7). Plane-wave (PW) pseudopotential calculations (pw.x code) were performed using LDA PAW pseudopotentials from the Pslibrary 1.0.0.
[56] Timròv, I., Marzari, N., and Cococcioni, M., *Phys. Rev. B*, **103** (2021) 045141.
[57] Abrahams, E. and Si, Q., *J. Phys.: Condens. Matter*, **23** (2011) 223201.
[58] Yi, M. *et al.*, *Nature Commun.*, **6** (2015) 7777.